

On the Emergent Spectra of Hot Protoplanet Collision Afterglows

Eliza Miller-Ricci

Harvard-Smithsonian Center for Astrophysics, 60 Garden St. Cambridge, MA 02138

`emillerricci@cfa.harvard.edu`

Michael R. Meyer

*Institute for Astronomy ETH, Physics Department, HIT J 22.4, CH-8093 Zurich,
Switzerland*

Sara Seager

*Department of Earth, Atmospheric, and Planetary Sciences, Department of Physics,
Massachusetts Institute of Technology, 54-1626, 77 Massachusetts Ave., Cambridge, MA
02139*

Linda Elkins-Tanton

*Department of Earth, Atmospheric, and Planetary Sciences, Massachusetts Institute of
Technology, 54-824, 77 Massachusetts Ave., Cambridge, MA 02139*

ABSTRACT

We explore the appearance of terrestrial planets in formation by studying the emergent spectra of hot molten protoplanets during their collisional formation. While such collisions are rare, the surfaces of these bodies may remain hot at temperatures of 1000-3000 K for up to millions of years during the epoch of their formation (of duration 10-100 Myr). These objects are luminous enough in the thermal infrared to be observable with current and next generation optical/IR telescopes, provided that the atmosphere of the forming planet permits astronomers to observe brightness temperatures approaching that of the molten surface. Detectability of a collisional afterglow depends on properties of the planet's atmosphere – primarily on the mass of the atmosphere. A planet with a thin atmosphere is more readily detected, because there is little atmosphere to obscure the hot surface. Paradoxically, a more massive atmosphere prevents one from easily seeing the hot surface, but also keeps the planet hot for a longer time. In terms of planetary mass, more massive planets are also easier to detect than smaller ones because of their larger emitting surface areas – up to a factor of 10

in brightness between 1 and 10 M_{\oplus} planets. We present preliminary calculations assuming a range of protoplanet masses (1-10 M_{\oplus}), surface pressures (1-1000 bar), and atmospheric compositions, for molten planets with surface temperatures ranging from 1000 to 1800 K, in order to explore the diversity of emergent spectra that are detectable. While current 8- to 10-m class ground-based telescopes may detect hot protoplanets at wide orbital separations beyond 30 AU (if they exist), we will likely have to wait for next-generation extremely large telescopes or improved diffraction suppression techniques to find terrestrial planets in formation within several AU of their host stars.

Subject headings: planetary systems

1. Introduction

Recent estimates suggest that between 10-20% of Sun-like stars harbor gas giant planets with masses greater than 30% the mass of Jupiter and with orbits ranging from < 0.1 AU to beyond 20 AU (Cumming et al. 2008). Based on new discoveries of super-Earths with masses 3-30 times the mass of the Earth (e.g. Lovis et al. 2006; Udry et al. 2007; Mayor et al. 2009) we anticipate that such bodies might be even more common. We await confirmation of these ideas from enhanced radial velocity and microlensing surveys, as well as space-based transit missions such as CoRoT (Baglin 2003; Barge et al. 2005) and Kepler (Borucki et al. 2004; Basri et al. 2005). Recently, direct imaging surveys have produced the first widely-accepted images of extrasolar gas giant planets (Kalas et al. 2008; Marois et al. 2008), proving that direct detection is yet another viable planet detection method. In addition to providing estimates of temperature and luminosity (and thus constraints on radius), direct detection enables us to investigate the composition of the planetary atmosphere, complementary to studies of bulk composition. Furthermore, the radiant energy of planets at orbital radii beyond that where insolation dominates the energy budget, provides estimates of the internal energy of the planet. Together, these data provide a whole greater than the sum of their parts in constraining models of the formation, structure, and evolution of planets of all masses.

What are the prospects for directly imaging terrestrial planets like Earth? Space-based mission concept studies of 1-2 meter class telescopes are underway that could just barely detect an Earth around the nearest stars at visible wavelengths (e.g. Guyon et al. 2006). Extremely large ground-based telescopes of the future likewise have the angular resolution to see planets around the nearest stars in the thermal infrared. Someday, ambitious space missions like Darwin/TPF will provide images and spectra of Earth-like planets around dozens of carefully chosen targets that will revolutionize our understanding of whether planetary

systems like our own (and the potential for life that such systems represent) are common or rare in the Milky Way.

An intriguing near-term possibility is to search for hot protoplanets during their epoch of formation, as originally proposed by Stern (1994). Zahnle et al. (2007) present a scenario for the early evolution of the Earth after the Moon-forming impact, thought to be the last of a series of giant impacts that built the Earth from a swarm of protoplanets (Stevenson 1987; Kenyon & Bromley 2004, 2006). Such impacts could impart enough energy on the forming protoplanet to render its surface molten. Indeed, a 1500 K molten body of one Earth radius is more than 600 times more luminous than the Earth, with a thermal emission spectrum peaking at wavelengths beyond 2 microns. The radiative lifetime of such a body in free space - if its atmosphere is completely blown off during the collision - is short ($< 100,000$ yrs; Stern 1994) compared to the expected age of such objects (1-100 Myr; Chambers 2001). However, such hot protoplanets may be observable if the molten magma ocean phase of the young forming protoplanet can last long enough. A long-lived magma ocean requires an atmosphere to slow down cooling - possible if the protoplanet retains a primordial atmosphere (Genda & Abe 2003) or can release a volatile atmosphere through outgassing (Elkins-Tanton 2008). With an atmosphere, the planetary surface could remain molten for durations of up to millions of years.

Whether or not a substantial fraction of any pre-existing atmosphere remains after a large collision is debated (Okeefe & Ahrens 1977; Genda & Abe 2003). However, recent work by Elkins-Tanton et al. (2003) and Elkins-Tanton (2008) describes a second longer-lasting magma ocean phase that is naturally accompanied by a thick atmosphere. It is this phase that dominates the timescale for how long the planet remains hot. The first magma ocean phase results from the energy imparted during the giant impact process. As the planet cools, the magma ocean solidifies, and volatile elements are released to form a new planetary atmosphere on timescales on the order of 100,000 years. This solidification process is by its nature gravitationally unstable. The magma ocean solidifies from the bottom upwards, and because the lighter element Mg is preferentially included in solid-forming minerals over the heavier element Fe, the solidifying magma ocean is less dense at the bottom and more dense at the top. This gravitational instability results in a fast overturning of the mantle, provided that the planet mass is larger than a lunar mass, and the magma ocean contains more than about 4 mass percent iron, as likely occurred in solar system terrestrial planets. As the hot, low-density material begins to rise, it experiences adiabatic decompression causing the mantle to remelt - once again forming a magma ocean. This is the second magma ocean phase, and this time the freshly molten planet is able to retain its high temperature over much longer timescales, due to the insulating effects of the outgassed atmosphere. This second molten phase can persist for several to ten million years depending on the planet

mass and composition of the outgassed atmosphere (Elkins-Tanton 2008).

If, as we expect, forming terrestrial planets are built through giant impact collisions, several post-impact magma ocean phases per protoplanet are likely. And if each planetary system produces multiple terrestrial or super-Earth systems (such as HD 40307, HD 69830, or the Solar System), we might hope to catch an Earth-like planet in a molten phase. A typical system with 2 super-Earths, each experiencing 2 giant impacts during formation that result in magma ocean phases lasting 2 million years each, will potentially be observable for 8 million years out of the 10-100 Myr years thought required to build terrestrial planets (O’Brien et al. 2007) – consistent with the timing of the Moon-forming impact from recent Hf-W chronologies (Kleine et al. 2008, see also Jacobsen et al. submitted). This calculation results in a 10% chance to observe such an event if the estimates of the frequency and duration of events are accurate. Indeed, Mamajek & Meyer (2007) explore the hypothesis that the enigmatic low-luminosity companion to 2MASS 1207a is in fact a hot protoplanet collision afterglow. In that case, the (improbable) hypothesis explored is that of a collision between a $7 M_{\oplus}$ projectile and a $70 M_{\oplus}$ target at 55 AU orbiting a 5-10 Myr brown dwarf found in a young cluster.

The presence of a hot molten surface however is a necessary but not sufficient condition for detection. Atmospheric windows must be present in the planet’s emitted spectrum that enable astronomers to observe brightness temperatures approaching that of the planetary surface. Addressing this issue is the subject of the present work. We present calculations of the emergent spectrum of a hot protoplanet with a molten surface, exploring a range of planet masses, atmospheric mass fractions, atmospheric compositions, and surface temperatures. We pay particular attention to the ground-based astronomical windows in the near-infrared where current and future telescopes capable of detecting these hot protoplanet collision afterglows are expected to be particularly effective. Our calculations suggest that, even in the most favorable assumptions, hot young planets are likely not detectable by current instruments on existing telescopes. However, instrumentation and space observatories under construction should be able to detect a subset of such objects on orbits beyond 20 AU (if they exist in sufficient numbers), while the next generation of extremely large telescopes will survey orbits comparable to the terrestrial planets in our solar system.

2. Methodology

2.1. Range of Planetary Parameters Considered

A handful of super-Earths in the 1-10 M_{\oplus} range have already been discovered, and it is expected that many more will be reported in the coming years. Observational constraints on super-Earth atmospheres however are not yet available. In the absence of a large statistical sample, we consider super-Earths with atmospheres covering a wide range of parameter space that could be expected for such planets. In terms of planetary mass, we consider super-Earths of 1, 5, and 10 M_{\oplus} . Assuming they have a similar composition to that of the Earth (67.5% silicate mantle and 32.5% iron core), these planets will have corresponding surface gravities, g , of approximately 9.8, 21.8, and 29.6 m/s^2 according to theoretical mass-radius relationships for solid exoplanets (Seager et al. 2007). These values for g depend on the assumed composition of the solid portion of the planet but only vary by up to 40% if vastly different compositions are employed such as pure water or pure iron.

The atmospheric composition of a super-Earth depends strongly on the conditions leading to its creation. Factors such as accretion and outgassing history, which are difficult to constrain with models, will ultimately determine the composition (Elkins-Tanton & Seager 2008). Additionally, molecular abundances in the atmosphere can be further altered through processes such as photochemistry, atmospheric escape, and interactions between the atmosphere and the planetary surface. For this reason we choose to examine the spectral signatures of a range of atmospheres that span the possible outcomes from outgassing and accretion scenarios. The atmospheres we consider are:

1. *Solar Composition Atmosphere* – This is our benchmark case, which represents either the remains of an initial accreted atmosphere or a hydrogen-rich outgassed atmosphere. We employ solar elemental abundances (Asplund et al. 2005) and assume that the molecular constituents reside in a state of chemical equilibrium (see Section 2.2). The resulting atmosphere is composed by volume of 85% H_2 , 15% He, and 560 ppm H_2O . At the temperatures that we are considering, this atmosphere bears strong similarities to a brown dwarf, although the surface gravity here is far lower.
2. *30 \times Solar Enhanced Metallicity Atmosphere* – This case is similar to scenario 1, but here the abundances of all elements other than hydrogen and helium have been enhanced to 30 times that of the Sun resulting in an atmosphere that is 81% H_2 , 15% He, and 1.7% H_2O .
3. *90% Water (steam), 10% CO_2 Atmosphere* – This atmosphere, as well as the next two that follow, represents the possible compositional outcome of an outgassing scenario.

H₂O-CO₂ atmospheres are expected to result naturally from surface outgassing as the planet cools. However, the exact ratio of H₂O to CO₂ depends strongly on the initial volatile content of the hot protoplanet (Elkins-Tanton & Seager 2008). The three outgassing scenarios on this list – scenarios 3, 4, and 5 – encompass a probable range of H₂O-CO₂ atmospheres that may occur.

4. *50% Water (steam), 50% CO₂ Atmosphere*
5. *10% Water (steam), 90% CO₂ Atmosphere*
6. *Venus-Composition Atmosphere* – This atmosphere has a composition mirroring that of Venus’ atmosphere and could be obtained either by outgassing or by accretion with subsequent escape of light-weight elements. Here the atmosphere is composed predominantly of CO₂ – 96.5% by volume – along with 3.5% N₂ and 20 ppm H₂O (Lewis 1995).

Protoplanet collision afterglows will only be observable in cases where the heat flow from the planet’s interior is sufficient to sustain a high emergent flux from the top of the planetary atmosphere. This is likely to occur only when the mantle is in a low-viscosity state, requiring a full to partial melt of the mantle. For this reason, we consider surface temperatures that are indicative of a molten planetary surface. Immediately after overturn the surface temperature of a (1 M_⊕) terrestrial planet will vary from ~ 3000 - 1500 K, and will slowly cool from there, becoming solid around 1000 K (Elkins-Tanton 2008). The more massive the planet, the hotter the solidus temperatures become at depth. There is some evidence that at depth silicate liquids become denser than their coexisting solids (Stixrude & Karki 2005), a condition that would mark the bottom of the magma ocean that would later interact with the surface. This may limit the temperature of overturning mantle materials to about 4000 K, even for the most massive super-Earths. Following the mantle overturn, the surface cools over millions of years through 1000 K, at which temperature an Earth-like composition would be solid. We produce emergent spectra from the intermediate to low end of the molten temperature range, where the planets will spend most of their time as they cool. The four surface temperatures that we consider are 1800, 1500, 1200, and 1000 K. It serves pointing out that we are considering only rocky terrestrial planets here and not ice planets, which would form outside of the snow line and then potentially migrate inwards. These planets would also experience similar protoplanet collisions, and whether or not they retain high enough brightness temperatures to be observable will depend strongly on how much energy is imparted in the collision and how quickly this energy is reradiated to space.

The surface pressure conditions for protoplanet collision afterglows are difficult to ascertain, since the pressure is dependent on atmospheric mass, which is not known *a priori* and

is strongly model dependent. Outgassed atmospheres of super-Earths may be able to attain very high surface pressures of up to several thousand bars (Elkins-Tanton & Seager 2008), depending on their exact histories and the volatile content upon formation. We therefore produce spectra for atmospheres covering a range of probable surface pressures – 1, 10, 100, and 1000 bars.

2.2. Description of the Model Atmosphere

To determine the emitted protoplanet spectra we place a simple model atmosphere on top of the hot molten planetary surface. Our atmosphere model follows the one developed in Miller-Ricci et al. (2009) but differs in that here the atmosphere is almost entirely heated from below by the planet’s hot surface rather than by the irradiation from the host star. The atmosphere that we consider is a grey gas in hydrostatic equilibrium. The temperature structure is then given by

$$T^4 = \frac{3}{4}T_{eff}^4\left(\tau + \frac{2}{3}\right), \quad (1)$$

where τ is the optical depth, and T_{eff} is the planet’s effective temperature. The pressure structure is determined by integrating the equation of hydrostatic equilibrium:

$$\frac{dP}{d\tau} = \frac{g}{\kappa_{gr}}, \quad (2)$$

where g is the surface gravity and κ_{gr} is the mean opacity in units of cm^2/g , based on the chemistry that we have employed. We calculate Rosseland mean opacities at depth but switch to Planck mean opacities for $\tau \ll 1$. Convection is included in the lower atmosphere, by switching to an adiabatic temperature-pressure profile in regions that are convectively unstable. For our entire calculation we assume an ideal gas equation of state (EOS), despite the fact that water is known to deviate from an ideal gas – particularly at high pressures and abundances. For the hot protoplanet we specify our desired surface temperature and pressure as boundary conditions, and then adjust T_{eff} and the upper limit on the optical depth scale (τ_{surf}) until they agree with those conditions. The other free parameters, g and κ_{gr} are specified by the model assumptions – the mass and radius of the planet and its atmospheric composition (see Section 2.1, above).

After determining the temperature-pressure profile, we calculate the planet’s emitted spectrum – at a resolution of 1,000 – by integrating the equation of radiative transfer through the planet’s atmosphere. The emergent intensity, I is given by

$$I(\lambda, \mu) = \frac{1}{\mu} \int_0^\tau S(T) e^{-\tau'/\mu} d\tau', \quad (3)$$

where S is the source function (assumed here to be Planckian), μ is the cosine of the viewing angle, and τ is the optical depth at the base of the atmosphere. We have tested this scheme to reproduce Earth’s and Venus’ emitted spectra, given their known T-P profiles and simulating Venus’ opaque H_2SO_4 cloud deck by cutting off the planetary emission at an altitude of 70 km above the surface. Our resulting spectra are in agreement with the observed planet-averaged emission for both of these cases (Moroz et al. 1986; Christensen & Pearl 1997) to within a factor of several to ten percent – sufficient for modeling the observational signals of extrasolar planet atmospheres – although difficulties remain for models to exactly reproduce Venus’s IR spectrum (e.g. Pollack et al. 1993) (see Figure 1).

In computing the emergent spectra, we include the dominant sources of molecular line opacity from 0.1 to 100 μm in the IR – CH_4 , CO (Freedman et al. 2007, and references therein), CO_2 (Rothman et al. 2005), and H_2O (Freedman et al. 2007; Partridge & Schwenke 1997). For the line profiles, we employ a Voigt broadening scheme. In addition to the line opacities, for a Venus-like atmospheric composition (case 6 above) CO_2 - CO_2 collision induced opacities become important, and without them the CO_2 line opacities imply the presence of wide transparent windows in the near-IR. Unfortunately, a full prescription for CO_2 - CO_2 collision induced opacities is not available in the literature, and we instead interpolate between near-IR laboratory measurements at 2.3 μm (Brodbeck et al. 1991) and theoretical calculations for wavelengths longward of 40 μm (Gruszka & Borysow 1997).

For the solar and enhanced metallicity atmospheres (cases 1 and 2) we determine molecular abundances in chemical equilibrium, starting from the initial elemental abundances for these two cases. Chemical equilibrium should be a reasonable assumption here given the high temperatures in the lower atmosphere, implying that reactions will occur quickly and will not be limited by temperature. However, in the absence of effective mixing, photochemical processes may drive the composition away from equilibrium in the upper atmosphere. For the equilibrium calculation, we perform a minimization of Gibbs free energy for 172 gas phase molecules and 23 atomic species, following the method outlined in White et al. (1958). The Gibbs free energy of each molecule as a function of temperature is parameterized by a polynomial fit from Sharp & Huebner (1990), which we have found to be well-matched to data from the NIST JANAF thermochemical tables (Chase 1998) over our temperature range of interest of 200-1500 K. We do not include condensed species in our equilibrium chemistry model, however for each atmosphere scenario we do check whether the temperature-pressure profile for each major species crosses into the regime where condensation and cloud formation would be expected.

3. Hot Protoplanet Emission Spectra

3.1. Main Results

The emergent spectra for hot protoplanets with 1500 K T_{surf} are shown in Figure 2 (in terms of brightness temperature) and Figure 3 (in terms of flux for a planetary system at a distance of 30 pc). There are spectral windows where the modeled fluxes are quite high, and the potential exists to observe brightness temperatures up to the planet’s surface temperature. However, this is generally only the case for the thinnest atmospheres and even then only in fairly narrow atmospheric windows.

For more massive atmospheres, the planet’s brightness temperature drops off quickly due to increased surface obscuration by a larger optically thick atmosphere. For atmospheres with kilobar surface pressures, the maximum brightness temperature that can potentially be observed for any of the atmospheric compositions we have considered is approximately 1000 K for planets with 1800 K surface temperatures and only 500 K for planets with 1000 K T_{surf} . Unfortunately, planets with thin atmospheres are also expected to retain their molten surfaces for the shortest periods of time. More massive atmospheres serve to prevent the escape of heat from the planetary surface and can therefore maintain high surface temperatures for up to several million years (Elkins-Tanton 2008). This is a dilemma, as the atmospheres that are the easiest to detect owing to their high brightness temperatures will potentially be the least likely to be observed due to their short lifetimes.

The effect of planetary mass on the emitted spectra is more subtle than that of surface pressure. According to Figure 2, the 10 M_{\oplus} planets emit at slightly higher brightness temperatures than the corresponding 1 M_{\oplus} planets – at all wavelengths. This effect ultimately results from the higher surface gravity and correspondingly smaller pressure scale height on the more massive super-Earth. For a given surface pressure, as the mass of the planet increases, the thickness of the atmosphere that the observer must “look through” to see the planetary surface drops off – explaining the somewhat higher brightness temperatures for more massive planets. However, for a given mass of atmosphere, the surface pressure will be higher on more massive planets owing to their correspondingly higher surface gravities. In terms of emergent flux, the more massive super-Earths are clearly more readily observable (Figure 3) because they emit from a larger surface area. The emitted fluxes are therefore weakly dependent on the composition of the planet itself, owing to its effect on the planetary radius. Here we have employed values of 1, 1.5, and 1.8 R_{\oplus} for the 1, 5, and 10 M_{\oplus} planets, respectively, corresponding to a planetary composition similar to that of the Earth.

Figure 4 shows the dependence of the emergent spectrum on the planet’s surface temperature for the case of a 1-bar solar-composition atmosphere. As expected, the brightness

temperature is strongly dependent on the surface temperature, with hotter planets emitting higher fluxes. Generally, for all of the atmospheres we have studied, planets with surface temperatures of 1500, 1200, and 1000 K emit at brightness temperatures that are up to 20%, 40%, and 50% reduced relative to that of an 1800 K T_{surf} planet. This is in line with an expectation that the planet’s brightness temperature should scale linearly with surface temperature, as a direct consequence of Equation 1

3.2. Description of the Spectra

3.2.1. Cases 1 and 2 – Solar Composition and Enhanced Metallicity

For the solar composition and enhanced metallicity atmospheres (scenarios 1 and 2 from Section 2.1), spectral features mostly result from water absorption bands. Additionally, in chemical equilibrium, the main carbon-bearing species expected for these atmospheres is methane, which reveals itself through absorption features in the spectra at both 2.2 and 3.4 microns. As an atmospheric constituent, methane is particularly susceptible to UV photodissociation. Depending on the planet’s proximity to the host star and the properties of the stellar UV emission, methane may or may not be stable in the hot super-Earth atmosphere. Additionally, the presence or absence of methane depends strongly on the ratio of its photodissociation rate to the rate of return reactions in the planetary atmosphere, which is strongly temperature dependent. The spectral features at 2.2 and 3.4 microns can therefore be used to diagnose whether or not methane is present in a hot super-Earth atmosphere, but it would not be surprising to find this molecule out of equilibrium.

If methane is successfully destroyed, the resulting carbon atoms will reform into the more photochemically stable molecules CO and CO₂. Even in a state of chemical equilibrium, the enhanced metallicity atmosphere may contain enough CO₂ for its spectral fingerprint to be observable at 4.3 μm , as is the case for the 1-bar atmosphere – see Figure 2. While CO is expected to be present in these atmospheres at abundances 100 times greater than that of CO₂ (up to 1ppm), it does not display any strong absorption bands shortward of 4.5 μm in these models.

3.2.2. Cases 3, 4, and 5 – H₂O - CO₂ Atmospheres

The spectra for the three outgassed atmosphere scenarios – 3, 4, and 5 – all strongly resemble one another owing to saturation of the water vapor and CO₂ lines at lower partial pressures than the ones considered here. This is despite the fact that the CO₂ abundance

increases from 10% to 90% and the H₂O abundance correspondingly decreases from 90% to 10% across these three cases. For cases 3, 4, and 5, the spectra reveal absorption features of both water and CO₂. Absorption bands at 1.1, 1.4, and 1.9 μm all result from water, while the band at 4.3 μm is due to CO₂. The additional absorption feature around 2.7 μm results from overlapping H₂O and CO₂ bands. Due to the strong spectral features at such high abundances of water and CO₂, an atmosphere composed of these two molecules should be readily identifiable. However, discerning the exact abundances of H₂O and CO₂ from emission spectra is more difficult, since the changes in the features are those realized in the non-linear wings of the absorption profiles.

3.2.3. Case 6 – Venus Composition

Hot super-Earth atmospheres of Venus-like composition (scenario 6 from Section 2.1) achieve high brightness temperatures, approaching that of the planetary surface, across large portions of the IR spectrum. For this reason, Venus-composition atmospheres probably have the best chance of being observed from the ground, although escape of flux through the transparent atmospheric windows will result in these planets cooling more quickly than some of the other composition scenarios. Since these atmospheres are composed predominantly of CO₂, their molten surfaces are not obscured by strong water absorption bands in the near-IR. The primary spectral features for a Venus-like atmosphere result from CO₂, but there are large windows between absorption bands from 2 to 2.5 microns and from 3 to 4 microns where an observer could potentially detect emission from the planetary surface. In between the CO₂ absorption bands the main source of opacity is collisional. As mentioned above in Section 2.2, a full characterization of CO₂ - CO₂ collision induced opacities is not available in the literature, and we have therefore interpolated between the only two available datasets. Artifacts as a result of this interpolation can be seen in the bottom right hand panel of Figure 2 with the flat “ceiling” in all of the spectra. It is possible that the true values for the CO₂-CO₂ collision induced opacities in this wavelength range could be quite different from the ones we have used for this study. However, additional laboratory experiments will clearly be necessary to resolve this issue.

3.3. The Effect of Clouds

The spectra presented in Figures 2 and 3 are all for cloud-free atmospheres. However, the presence of clouds can further affect the observability of a molten super-Earth by preventing the escape of flux from the planet’s hot surface. Generally, if clouds are present,

the atmosphere will emit radiation at or below the temperature of the cloud deck. Venus is an good example of this effect, where the planetary surface is very hot, but the IR emission from the planet occurs at a much lower temperature owing to the fact that most of the flux emitted at the surface does not escape through Venus’ sulfuric acid cloud layer.

For the atmospheric scenarios that we present here, the temperatures are too high for CO₂ clouds to form. However, water clouds are a possibility in a number of cases. One-dimensional models like the one we present here have a limited ability to properly account for the presence of clouds. For example, a 1-D model would predict water clouds on Earth, but it would not correctly predict that these clouds are patchy and do not entirely obscure the surface of the Earth at any given time. In our model we determine if water clouds are present by comparing the temperature-partial pressure curve for H₂O against its condensation curve. If the two curves intersect, we assume that clouds can form at the lowest location in the atmosphere where water will condense.

We find that most of the atmosphere scenarios with high abundances of water have the potential to form clouds. For atmospheric composition scenarios 1, 2, 3, 4, and 5 (from Section 2.1), clouds will form for 100- and 1000-bar atmospheres (as well as for 10-bar atmospheres in scenarios 2, 3, and 4) at temperatures below 320 K and pressures below 0.1 bars. If these clouds are thick and entirely blanket the planetary surface, then the observability of these planets will be severely limited due to their resulting low brightness temperatures. However, if the clouds only obscure a fraction of the planet, quite high planet-averaged brightness temperatures can still be achieved. This is shown in Figure 5 where we plot full- and partial-cloud cover spectra for all of the atmospheres where clouds are a possibility. The presence of clouds does have an interesting additional consequence in that clouds can essentially insulate the planet, allowing the planetary surface to remain molten for much longer than it would be able to otherwise.

4. Observational Implications

4.1. Prospects With Current Telescopes

Given these results, we now explore the prospects of detecting hot protoplanet collision afterglows with current instrumentation and offer ideas concerning future search strategies. Several groups (e.g. Lafrenière et al. 2007; Biller et al. 2007; Kasper et al. 2007; Heinze et al. 2008) have published null results for solar-type stars based on high contrast imaging results in the near-infrared at 1.65 microns (H-band) and 3.6 microns (L-band). The goal of these surveys was to detect gas giant planets at large separations and place limits on the power-

law surface density of such companions, as well as on the outer limit of circumstellar planet formation, based on extrapolation of results from radial velocity surveys (e.g. Cumming et al. 2008). Results to date suggest that massive gas giant planets ($> 3 M_J$) do not form frequently at separations beyond 20 AU, compared to gas giants at smaller separations. The question then arises - could such surveys have detected the hot protoplanet collision afterglows, given the model spectra described above?

Forming super-Earths with extremely tenuous atmospheres (the 1 bar models of Figure 2) would be detectable if they lurk at large enough angular separations. For example, the H-band observations of Lafrenière et al. (2007) from the Gemini Deep Planet Survey are limited by the contrast of any potential planet against the glare of the central Sun-like star at separations within several arcseconds. In order to detect a $2 R_{\oplus}$ hot protoplanet in formation, with a solar composition and a 1 bar atmosphere, a contrast of 14.3 magnitudes is required in the H-band. Lafrenière et al. (2007) achieve this contrast at a typical angular separation of 1.5 arcseconds. The youngest targets in their sample (with ages less than 100 Myr) have typical distances of 30 pc. As a result, these observations are sensitive to hot protoplanet collision afterglows on physical scales greater than 45 AU in these systems.

For comparison, the L-band observations taken at the VLT as reported by Kasper et al. (2007) reach the thermal background limit (rather than being contrast-limited) at angular separations greater than 1.5 arcseconds. This corresponds roughly to 10 times the classical Rayleigh diffraction-limit. The background limit reached in 15-20 minutes of on-source integration time was $L < 16$ magnitude. Based on the models presented above, a $2 R_{\oplus}$ hot protoplanet collision afterglow would have an absolute L-band magnitude of 15.5 corresponding to a distance of 10 pc while a forming $1 R_{\oplus}$ planet would have $M_L = 17$ magnitudes. As the targets in their survey range in age from 10-30 Myr with distances from 10-50 pc they could have in principle detected protoplanets in formation beyond 15 AU for their nearest targets or hot planets as large as Uranus (although such planets would probably not be primarily composed of molten rock) out to distances of 30 pc at orbital distances beyond 45 AU.

No extremely faint common proper motion companions have been detected in any of these surveys, perhaps indicating that in addition to gas giant planets, the formation of super-Earths at large distances from their host stars may be rare as well. This would not be surprising, considering that planet formation through giant impact accretion is expected to be inefficient at the large orbital separations probed by current surveys. Additionally, as mentioned above in Section 3.1, Elkins-Tanton (2008) points out that there is a relationship between the length of time a forming planet's surface remains molten and the density of its insulating atmospheric blanket. Those protoplanets with thin atmospheres (1-100 bars)

retain surface temperatures above 1000 K only a little longer than the thermal cooling time (approximately 10,000 yrs). Protoplanets with dense atmospheres will remain molten for up to 100 times longer. Yet it is precisely these planets that are difficult to detect as the observable brightness temperatures are factors of 2-4 cooler than the surface temperatures (see Figure 2). For example, even a 10-bar atmosphere, which does not appreciably affect the cooling time, would be about 1.5 magnitudes fainter for both a 1 and 10 M_{\oplus} planet with a solar composition atmosphere. The difference is even worse for the 30 \times solar composition atmosphere, but not as bad for the various H₂O and CO₂ mixtures considered above. Venus composition is most favorable in this regard – even a 1000-bar atmosphere is only 3.7 magnitudes fainter in both the H- and L-bands. However a Venus-composition atmosphere will cool more quickly than the other compositional scenarios since it lacks the greenhouse trap of water vapor.

Given the ratio of cooling time to age, we would need a sample of thousands of stars to see just one protoplanet collision afterglow with current instrumentation. Even then, successful detection would rely on the presence of collisional afterglows at large orbital separations (> 45 AU) – an implausible scenario. However, prospects for detections are far better with future instrumentation, as described below.

4.2. Prospects With Future Instrumentation

Graham et al. (2007) describe the capabilities of Gemini Planet Imager (GPI) under development for the 8 meter Gemini telescopes. They expect to achieve extraordinary contrasts of more than 21 magnitudes in the H-band at 0.5 arcsecond separations. This would permit detection of forming terrestrial planets of solar composition with ease at physical separations greater than 5-15 AU around the nearest targets. It could even probe systems with relatively dense atmospheres, greatly increasing the chance for detection as discussed above. Similar capabilities are planned for the VLT utilizing the Spectro-Polarimetric High-contrast Exoplanet REsearch (SPHERE) instrument (Beuzit et al. 2008). In the L-band, Kenworthy et al. (2007) describe the use of an apodizing phase plate to achieve diffraction suppression, enabling one to reach the background limit at $3 \lambda/D$ rather than $10 \lambda/D$. This would improve the inner working angle and thus the physical resolution of existing surveys using current 6-10 meter telescopes by a factor of three. Future work with the Large Binocular Telescope (Hinze et al. 2008) would enable these techniques to be used with the 23 meter baseline of the Fizeau interferometer. This could provide physical resolution within a few AU for the nearest targets using the LMIRCam instrument now under construction (Wilson et al. 2008).

Further progress will be made with next-generation ground-based observatories. One

of the main science goals of future extremely large telescopes (ELTs) with planned mirror sizes of 25-50 m is to directly image extrasolar planets, perhaps even terrestrial planets. With the increased angular resolution resulting from their large diameters, planet imaging instruments on telescopes such as the Giant Magellan Telescope (GMT), the Thirty Meter Telescope (TMT), and the European ELT (E-ELT) will probe even smaller angular separations than is possible with current observing facilities. Near-infrared imagers on these telescopes, fed by extreme adaptive optics, would have the capability to detect planets within 0.1" of potential planet-hosting stars¹ (Macintosh et al. 2006; Kasper et al. 2008). This will allow astronomers to directly image planets within several AU of their host stars for the first time – a region where we know terrestrial planet formation was effective in our own solar system. Achievable contrasts for instruments such as HRCam on GMT, the Planet Formation Imager (PFI) on TMT, and the Exo-Planet Imaging Camera and Spectrograph (EPICS) on E-ELT are predicted to reach factors of 10^{-8} to 10^{-9} (> 20 mag) within 0.1" and remain contrast limited for Sun-like target stars within 50 parsecs (< 5 AU) for reasonable 6-10 hour integrations. This would permit detection of hot protoplanet atmospheres of up to 100 bars for $1 M_{\oplus}$ planets and potentially up to 1000 bars for $10 M_{\oplus}$ planets or for planets with surface temperatures exceeding 1500 K (see Figure 6). In the thermal infrared, diffraction suppression techniques currently being developed (e.g. Kenworthy et al. 2007) might enable background-limited performance without the use of extreme adaptive optics within $3 \lambda / D$. For the GMT, this would result in a survey depth of $L < 22$ magnitudes (5 sigma, 1 hr) within 0.1" (1-5 AU for the nearest targets from 10-50 pc), and could be improved upon even further for longer integration times.

ELTs should therefore be able to detect young forming super-Earths with thick atmospheres (of up to 1000 bars) within several AU of their host stars throughout the near-IR ground-based windows from 1-5 microns. With the $100 \times$ longer 'shelf-life' of these atmospheres (relative to more tenuous 1 bar atmospheres), one could reasonably expect 10 % of Sun-like stars with ages 10-100 Myr to have a planet in a molten surface phase at a given time. Thus for future ELTs, a sample of 100 targets within 50 pc could yield several hot protoplanet collision afterglow candidates. Multi-wavelength photometry and/or spectroscopy could then be used to determine both the temperature and luminosity of these objects, enabling estimates of their radii. Spectroscopic follow-up could also provide constraints on composition and surface gravity, further constraining their nature.

In terms of space-based observing, ten years from now JWST will be surveying nearby stars for planets at modest separation using a variety of direct imaging and coronagraphic

¹GMT Conceptual Design Report: <http://www.gmto.org/CoDRpublic>

techniques. The three imaging instruments (NIRCam, FGS/TFI, and MIRI) will have unmatched sensitivity to search for cool planets in the thermal infrared (Meyer et al. 2007). As a result, JWST will be unsurpassed at large separations (beyond 1”) limited only by the low background of a cooled space telescope. With 3.6 micron sensitivity of approximately $L < 26$ magnitude (10 sigma, 3 hr), NIRCam will be able to see 1 R_{\oplus} planets after impact with 1000 bar atmospheres, but only at separations > 20 AU for typical targets. If super-Earths in formation at separations beyond 15 AU are there to be found (which remains debatable) it may be that JWST, with its ability to detect even the faintest forming protoplanets with the densest atmospheres (and thus longest ‘shelf-life’ for detection), will find the first one.

5. Summary and Discussion

We have shown that hot protoplanet collisional afterglows may be observable from the ground with next generation ELT’s, under certain conditions described as follows. Generally, the most massive terrestrial planets will have the largest observable signals, due to their larger emitting surface areas. Planets of 10 M_{\oplus} can be up to a factor of 10 brighter than 1 M_{\oplus} planets in the near-IR. In terms of their atmospheres, hot young super-Earths with atmospheres of 1-1000 bars and surface temperatures greater than 1500 K will be detectable with next-generation ground-based facilities such as the GMT, TMT, and E-ELT. However, true Earth analogues (1 R_{\oplus}) planets with 1000-bar atmospheres may remain out of reach. Thick atmospheres have the advantage that they insulate the planetary surface from heat loss, allowing a super-Earth in formation to remain molten for up to millions of years. However, these planets will also be difficult to observe for the same reason – the blanketing atmosphere keeps the planetary surface hot by preventing large amounts of flux from escaping to space. Still, there is a compelling case to search for hot protoplanet afterglows with future telescopes and planet-finding instruments. If such protoplanet collision afterglows are successfully observed, they will allow astronomers to study formation mechanisms and occurrence rates for planets in the low-mass, terrestrial regime. As discussed above, successful detection of several protoplanet collision afterglow candidates with next-generation ELTs should require observations of a sample of ~ 100 young stars within 50 pc.

Once astronomers do succeed in imaging protoplanet collision afterglows, follow-up observations of these objects will additionally allow for characterization of their atmospheres. The bulk composition of super-Earth atmospheres is currently an open question, owing to the fact that no observations currently exist to constrain their properties. Theoretical models provide some insight into the expected range of atmospheric composition, but even these models produce a broad range of possible atmospheres (e.g. Elkins-Tanton & Seager 2008;

Genda & Abe 2003). Indeed, young super-Earths are likely host to a wide variety of atmospheres, with bulk compositions that depend strongly on the planet’s formation history. Fortunately, many of the planet imagers planned for next-generation telescopes are designed to have spectrographic capabilities – necessary for characterizing the atmospheres of these young protoplanets. However, one look at Figures 2-5 should be enough to convince the reader that there is significant degeneracy between the emergent spectra for the various atmosphere scenarios that we have proposed. Unambiguously determining the atmospheric composition, mass fraction, and surface temperature for a collisional afterglow will therefore require spectral observations taken at a high enough spectral resolution and signal-to-noise to break these degeneracies.

One particularly interesting question that could be addressed by spectral observations of super-Earth collision afterglows is to determine whether or not young silicate planets can form initially “dry” atmospheres (those without water). In the study of solar system planets, there is ongoing debate as to whether or not Venus formed dry (e.g. Lewis 1972; Grinspoon & Lewis 1988) or lost its hydrogen later in its lifetime due to photodissociation of water vapor and hydrodynamic escape (e.g. Kasting 1988). The atmosphere models presented in this paper produce markedly different spectra for a dry Venus-composition atmosphere and a wet atmosphere of 10% water. In particular, these spectra differ by factors of 10 or more in emitted flux in the wavelength ranges of 1.1-1.2, 1.3-1.5, 1.8-1.9, 2.4-2.6, and 3.0-3.4 μm . Observations taken in any of these wavebands at a signal-to-noise of several should therefore be sufficient to differentiate between wet and dry atmospheres, potentially allowing astronomers to determine whether dry atmospheres on young super-Earths are a possibility.

We would like to thank Bruce Macintosh for sharing his insight on exoplanet imaging techniques and Dan Fabricant for discussions of the imaging capabilities of the GMT. We also thank Phil Hinz, Scott Kenyon, and Eric Mamajek for useful discussions. MRM acknowledges the Harvard Origins of Life Initiative, the Smithsonian Astrophysical Observatory, and a NASA TPF Foundation Science Program grant NNG06GH25G (PI: S. Kenyon) for sabbatical support. LE-T acknowledges funding from the NSF astronomy program.

REFERENCES

- Asplund, M., Grevesse, N., & Sauval, A. J. 2005, in *Astronomical Society of the Pacific Conference Series*, Vol. 336, *Cosmic Abundances as Records of Stellar Evolution and Nucleosynthesis*, ed. T. G. Barnes, III & F. N. Bash, 25–+

- Baglin, A. 2003, *Advances in Space Research*, 31, 345
- Barge, P., Baglin, A., Auvergne, M., Buey, J.-T., Catala, C., Michel, E., Weiss, W. W., Deleuil, M., Jorda, L., Moutou, C., & COROT Team. 2005, in *SF2A-2005: Semaine de l’Astrophysique Francaise*, ed. F. Casoli, T. Contini, J. M. Hameury, & L. Pagani, 193–+
- Basri, G., Borucki, W. J., & Koch, D. 2005, *New Astronomy Review*, 49, 478
- Beuzit, J.-L., Feldt, M., Dohlen, K., Mouillet, D., Puget, P., Wildi, F., Abe, L., Antichi, J., Baruffolo, A., Baudoz, P., Boccaletti, A., Carbillet, M., Charton, J., Claudi, R., Downing, M., Fabron, C., Feautrier, P., Fedrigo, E., Fusco, T., Gach, J.-L., Gratton, R., Henning, T., Hubin, N., Joos, F., Kasper, M., Langlois, M., Lenzen, R., Moutou, C., Pavlov, A., Petit, C., Pragt, J., Rabou, P., Rigal, F., Roelfsema, R., Rousset, G., Saisse, M., Schmid, H.-M., Stadler, E., Thalmann, C., Turatto, M., Udry, S., Vakili, F., & Waters, R. 2008, in *Presented at the Society of Photo-Optical Instrumentation Engineers (SPIE) Conference*, Vol. 7014, *Society of Photo-Optical Instrumentation Engineers (SPIE) Conference Series*
- Biller, B. A., Close, L. M., Masciadri, E., Nielsen, E., Lenzen, R., Brandner, W., McCarthy, D., Hartung, M., Kellner, S., Mamajek, E., Henning, T., Miller, D., Kenworthy, M., & Kulesa, C. 2007, *ApJS*, 173, 143
- Borucki, W., Koch, D., Boss, A., Dunham, E., Dupree, A., Geary, J., Gilliland, R., Howell, S., Jenkins, J., Kondo, Y., Latham, D., Lissauer, J., & Reitsema, H. 2004, in *ESA SP-538: Stellar Structure and Habitable Planet Finding*, ed. F. Favata, S. Aigrain, & A. Wilson, 177–182
- Brodbeck, C., Nguyen, V.-T., Bouanich, J.-P., Boulet, C., Jean-Louis, A., Bezar, B., & de Bergh, C. 1991, *J. Geophys. Res.*, 96, 17497
- Chambers, J. E. 2001, *Icarus*, 152, 205
- Chase, M. W. 1998, *NIST-JANAF Thermochemical Tables* (4th ed.; Washington DC; Am. Chem. Soc.)
- Christensen, P. R. & Pearl, J. C. 1997, *J. Geophys. Res.*, 102, 10875
- Cumming, A., Butler, R. P., Marcy, G. W., Vogt, S. S., Wright, J. T., & Fischer, D. A. 2008, *PASP*, 120, 531
- Elkins-Tanton, L. & Seager, S. 2008, *ArXiv e-prints*, 808

- Elkins-Tanton, L. T. 2008, *Earth and Planetary Science Letters*, 271, 181
- Elkins-Tanton, L. T., Parmentier, E. M., & Hess, P. C. 2003, *Meteoritics and Planetary Science*, 38, 1753
- Freedman, R. S., Marley, M. S., & Lodders, K. 2007, *ArXiv e-prints*, 706
- Genda, H. & Abe, Y. 2003, *Icarus*, 164, 149
- Graham, J. R., Macintosh, B., Doyon, R., Gavel, D., Larkin, J., Levine, M., Oppenheimer, B., Palmer, D., Saddlemyer, L., Sivaramakrishnan, A., Veran, J.-P., & Wallace, K. 2007, *ArXiv e-prints*
- Grinspoon, D. H. & Lewis, J. S. 1988, *Icarus*, 74, 21
- Gruszka, M. & Borysow, A. 1997, in *American Institute of Physics Conference Series*, Vol. 386, *American Institute of Physics Conference Series*, 429–430
- Guyon, O., Angel, J. R. P., Bowers, C., Burge, J., Burrows, A., Codona, J., Greene, T., Iye, M., Kastig, J., Martin, H., McCarthy, Jr., D. W., Meadows, V., Meyer, M., Pluzhnik, E. A., Sleep, N., Spears, T., Tamura, M., Tenerelli, D., Vanderbei, R., Woodgate, B., Woodruff, R. A., & Wolf, N. J. 2006, in *Society of Photo-Optical Instrumentation Engineers (SPIE) Conference Series*, Vol. 6265, *Society of Photo-Optical Instrumentation Engineers (SPIE) Conference Series*
- Heinze, A. N., Hinz, P. M., Kenworthy, M., Miller, D., & Sivanandam, S. 2008, *ArXiv e-prints*
- Hinz, P. M., Bippert-Plymate, T., Breuninger, A., Connors, T., Duffy, B., Esposito, S., Hoffmann, W., Kim, J., Kraus, J., McMahan, T., Montoya, M., Nash, R., Durney, O., Solheid, E., Tozzi, A., & Vaitheeswaran, V. 2008, in *Society of Photo-Optical Instrumentation Engineers (SPIE) Conference Series*, Vol. 7013, *Society of Photo-Optical Instrumentation Engineers (SPIE) Conference Series*
- Kalas, P., Graham, J. R., Chiang, E., Fitzgerald, M. P., Clampin, M., Kite, E. S., Stapelfeldt, K., Marois, C., & Krist, J. 2008, *Science*, 13 November 2008 (10.1126/science.1166609)
- Kasper, M., Apai, D., Janson, M., & Brandner, W. 2007, *A&A*, 472, 321
- Kasper, M. E., Beuzit, J.-L., Verinaud, C., Yaitskova, N., Baudoz, P., Boccaletti, A., Gratton, R. G., Hubin, N., Kerber, F., Roelfsema, R., Schmid, H. M., Thatte, N. A., Dohlen, K., Feldt, M., Venema, L., & Wolf, S. 2008, in *Presented at the Society of Photo-Optical Instrumentation Engineers (SPIE) Conference*, Vol. 7015, *Society of Photo-Optical Instrumentation Engineers (SPIE) Conference Series*

- Kasting, J. F. 1988, *Icarus*, 74, 472
- Kenworthy, M. A., Codona, J. L., Hinz, P. M., Angel, J. R. P., Heinze, A., & Sivanandam, S. 2007, *ApJ*, 660, 762
- Kenyon, S. J. & Bromley, B. C. 2004, *ApJ*, 602, L133
- . 2006, *AJ*, 131, 1837
- Kleine, T., Touboul, M., van Orman, J. A., Bourdon, B., Maden, C., Mezger, K., & Halliday, A. N. 2008, *Earth and Planetary Science Letters*, 270, 106
- Lafrenière, D., Doyon, R., Marois, C., Nadeau, D., Oppenheimer, B. R., Roche, P. F., Rigaut, F., Graham, J. R., Jayawardhana, R., Johnstone, D., Kalas, P. G., Macintosh, B., & Racine, R. 2007, *ApJ*, 670, 1367
- Lewis, J. S. 1972, *Icarus*, 16, 241
- . 1995, *Physics and chemistry of the solar system* (San Diego: Academic Press, —c1995)
- Lovis, C., Mayor, M., Pepe, F., Alibert, Y., Benz, W., Bouchy, F., Correia, A. C. M., Laskar, J., Mordasini, C., Queloz, D., Santos, N. C., Udry, S., Bertaux, J.-L., & Sivan, J.-P. 2006, *Nature*, 441, 305
- Macintosh, B., Troy, M., Doyon, R., Graham, J., Baker, K., Bauman, B., Marois, C., Palmer, D., Phillion, D., Poyneer, L., Crossfield, I., Dumont, P., Levine, B. M., Shao, M., Serabyn, G., Shelton, C., Vaisht, G., Wallace, J. K., Lavigne, J. F., Valee, P., Rowlands, N., Tam, K., & D., H. 2006, in *Presented at the Society of Photo-Optical Instrumentation Engineers (SPIE) Conference, Vol. 6272, Society of Photo-Optical Instrumentation Engineers (SPIE) Conference Series*
- Mamajek, E. E. & Meyer, M. R. 2007, *ApJ*, 668, L175
- Marois, C., Macintosh, B., Barman, T., Zuckerman, B., Song, I., Patience, J., Lafrenière, D., & Doyon, R. 2008, *Science*, 13 November 2008 (10.1126/science.1166585)
- Mayor, M., Udry, S., Lovis, C., Pepe, F., Queloz, D., Benz, W., Bertaux, J.-L., Bouchy, F., Mordasini, C., & Segransan, D. 2009, *A&A*, 493, 639
- Meyer, M. R., The Nircam, & Fgs/Tfi Teams. 2007, in *In the Spirit of Bernard Lyot: The Direct Detection of Planets and Circumstellar Disks in the 21st Century*, ed. P. Kalas
- Miller-Ricci, E., Seager, S., & Sasselov, D. 2009, *ApJ*, 690, 1056

- Moroz, V. I., Linkin, V. M., Matsygorin, I. A., Spaenkuch, D., & Doehler, W. 1986, *Appl. Opt.*, 25, 1710
- O'Brien, D. P., Morbidelli, A., & Bottke, W. F. 2007, *Icarus*, 191, 434
- Okeefe, J. D. & Ahrens, T. J. 1977, *Science*, 198, 1249
- Partridge, H. & Schwenke, D. W. 1997, *J. Chem. Phys.*, 106, 4618
- Pollack, J. B., Dalton, J. B., Grinspoon, D., Wattson, R. B., Freedman, R., Crisp, D., Allen, D. A., Bevard, B., Debergh, C., Giver, L. P., Ma, Q., & Tipping, R. 1993, *Icarus*, 103, 1
- Rothman, L. S., Jacquemart, D., Barbe, A., Benner, D. C., Birk, M., Brown, L. R., Carleer, M. R., Chackerian, C., Chance, K., Coudert, L. H., Dana, V., Devi, V. M., Floud, J.-M., Gamache, R. R., Goldman, A., Hartmann, J.-M., Jucks, K. W., Maki, A. G., Mandin, J.-Y., Massie, S. T., Orphal, J., Perrin, A., Rinsland, C. P., Smith, M. A. H., Tennyson, J., Tolchenov, R. N., Toth, R. A., Vander Auwera, J., Varanasi, P., & Wagner, G. 2005, *Journal of Quantitative Spectroscopy and Radiative Transfer*, 96, 139
- Seager, S., Kuchner, M., Hier-Majumder, C. A., & Militzer, B. 2007, *ApJ*, 669, 1279
- Sharp, C. M. & Huebner, W. F. 1990, *ApJS*, 72, 417
- Stern, S. A. 1994, *AJ*, 108, 2312
- Stevenson, D. J. 1987, *Annual Review of Earth and Planetary Sciences*, 15, 271
- Stixrude, L. & Karki. 2005, *Science*, 310, 297
- Udry, S., Bonfils, X., Delfosse, X., Forveille, T., Mayor, M., Perrier, C., Bouchy, F., Lovis, C., Pepe, F., Queloz, D., & Bertaux, J.-L. 2007, *A&A*, 469, L43
- White, W. B., Johnson, S. M., & Dantzig, G. B. 1958, *J. Chem. Phys.*, 28, 751
- Wilson, J. C., Hinz, P. M., Skrutskie, M. F., Jones, T., Solheid, E., Leisenring, J., Garnavich, P., Kenworthy, M., Nelson, M. J., & Woodward, C. E. 2008, in Presented at the Society of Photo-Optical Instrumentation Engineers (SPIE) Conference, Vol. 7013, Society of Photo-Optical Instrumentation Engineers (SPIE) Conference Series
- Zahnle, K., Arndt, N., Cockell, C., Halliday, A., Nisbet, E., Selsis, F., & Sleep, N. H. 2007, *Space Science Reviews*, 129, 35

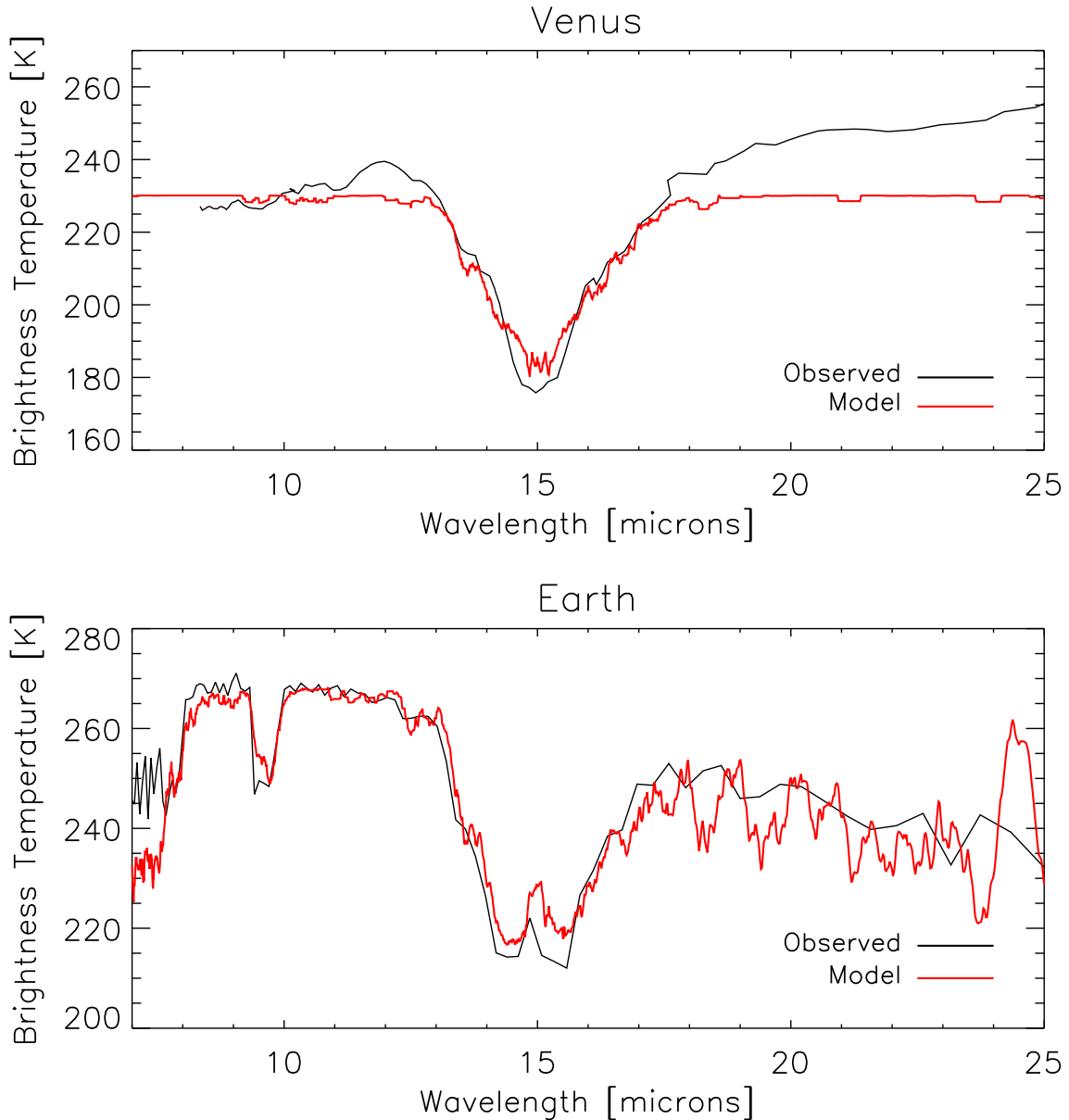


Fig. 1.— Tests of our model scheme to reproduce Venus’ (Moroz et al. 1986) and Earth’s (Christensen & Pearl 1997) emitted spectra. To simulate Venus’ sulfuric acid cloud layer, we cut off all emission below an altitude of 70 km ($T_B = 230$ K). This explains the mismatch between the model and the observations in the continuum at wavelengths longer than 18 μm , where the brightness temperature becomes as high as 255 K. For Earth we simulate the planet-averaged emission spectrum by averaging together a cloud-free model spectrum with a cloudy spectrum (emission cut off at a cloud deck of altitude 6 km), assuming that 59% of Earth’s surface is obscured by clouds. For both planets, our model reproduces the observations to within 10%, even in the continuum of Venus’ spectrum.

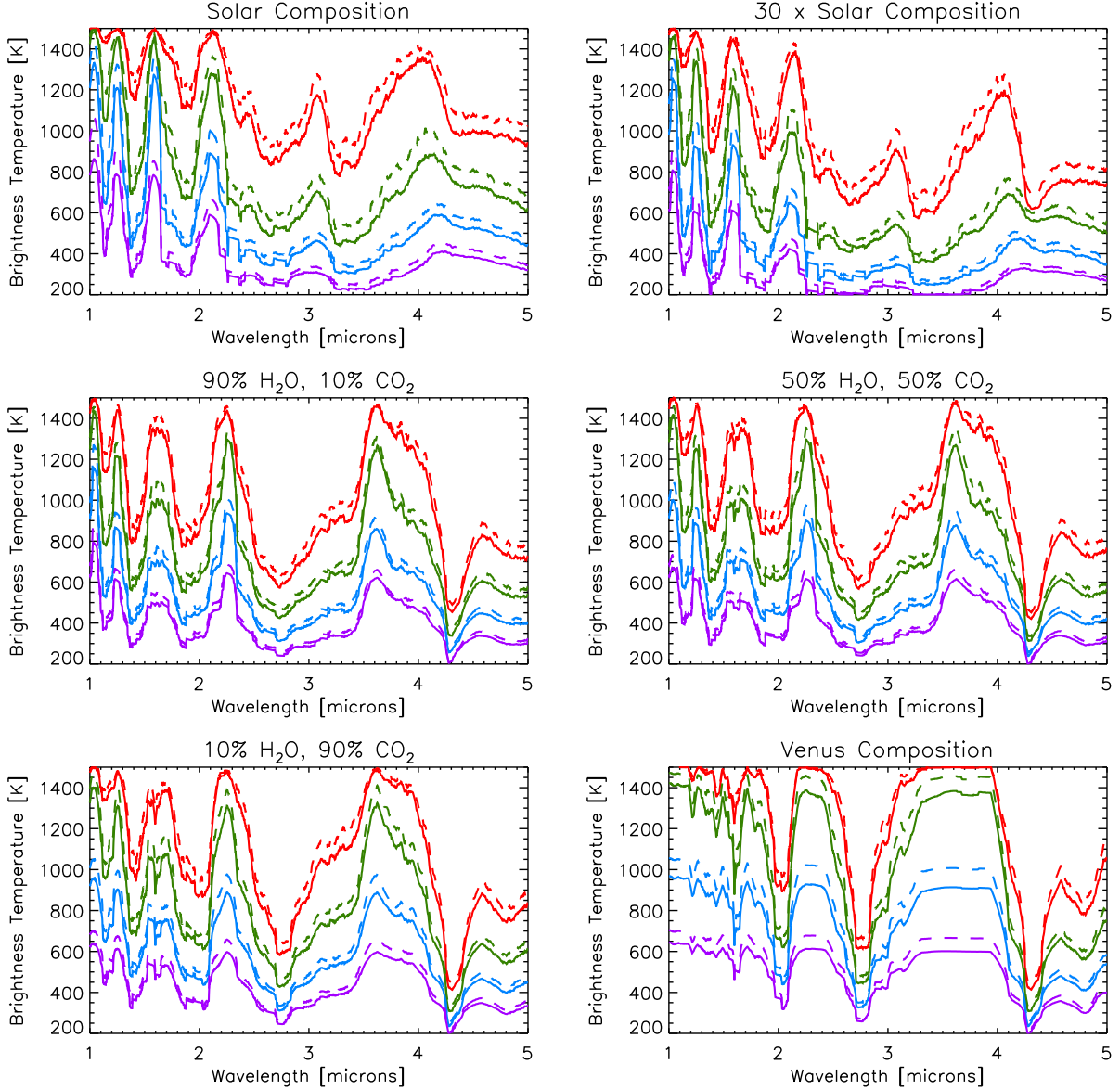


Fig. 2.— Spectra of hot molten super-Earths for 6 cases of atmospheric composition. All spectra are for planets with a 1500 K surface temperature. Planets with surface pressures of 1, 10, 100, and 1000 bars are denoted by red, green, blue, and purple lines respectively. Spectra for 1 M_⊕ planets are shown with solid lines and those for 10 M_⊕ planets with dashed lines. The spectra are dependent on the underlying temperature-pressure profile, and profiles other than a simple gray approximation may therefore alter the appearance of the spectra presented here.

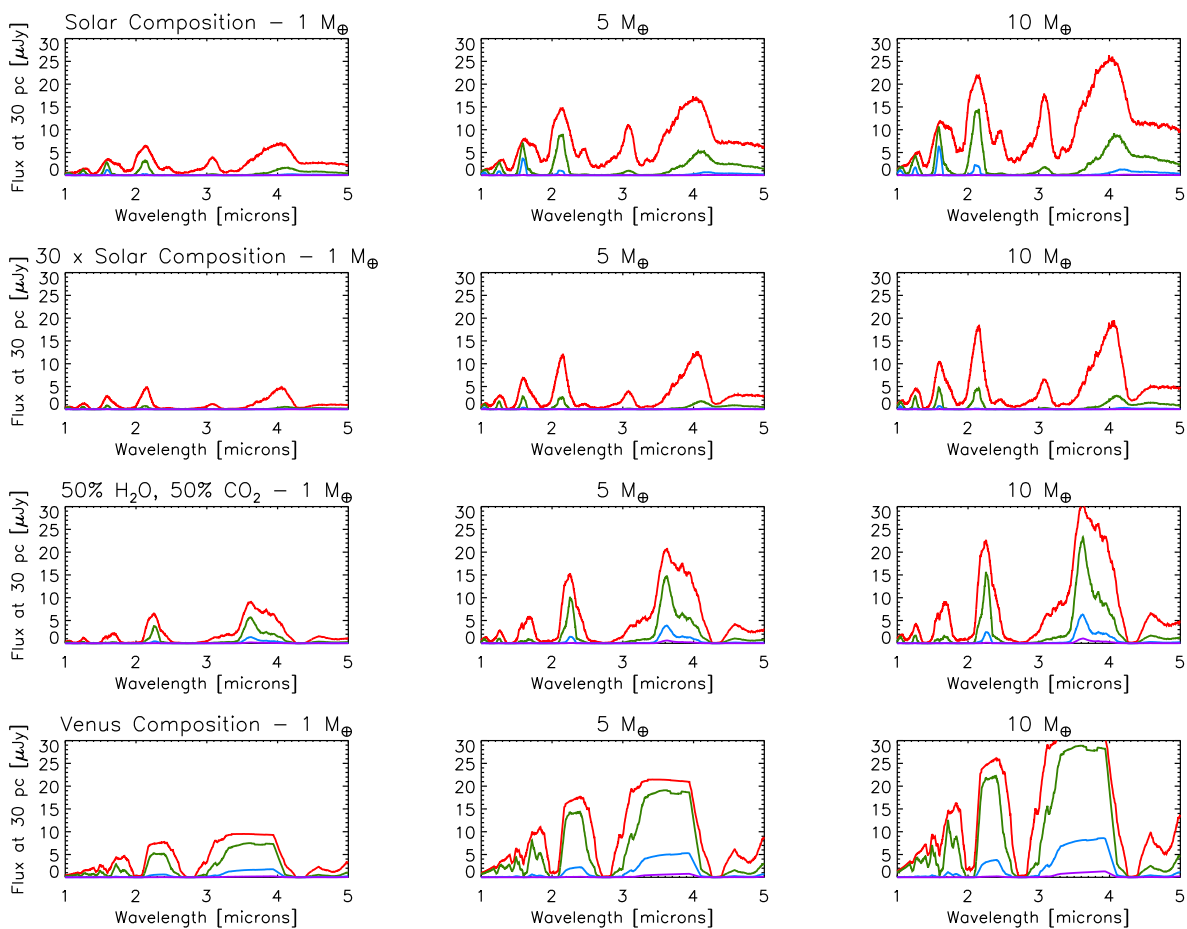


Fig. 3.— Spectra of hot molten super-Earths for 4 of the 6 cases of atmospheric composition in flux units. (Compositional scenarios 3 and 5 have been omitted here, as their spectra are quite similar to those of case 4 – 50% H_2O , 50% CO_2 .) The more massive planets give off higher overall fluxes due to their larger surface areas.

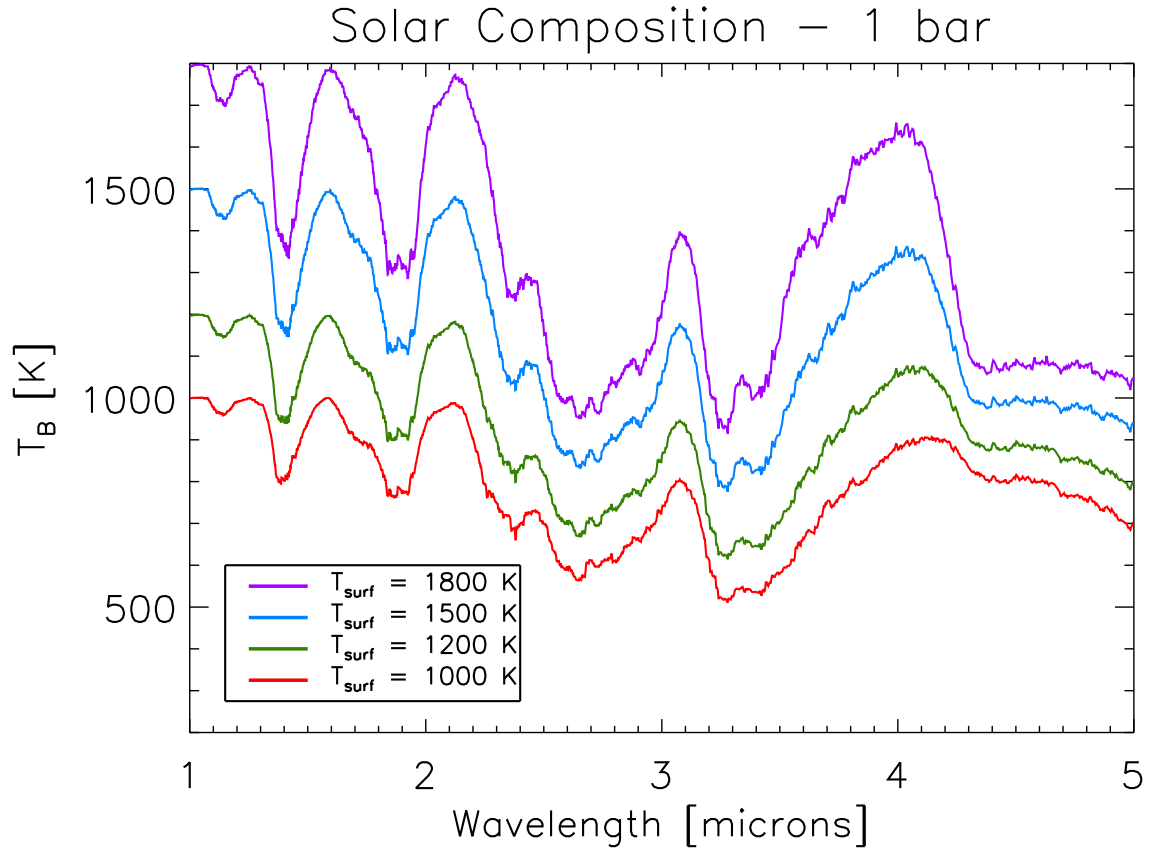


Fig. 4.— Sample spectra of hot molten super-Earths showing the dependence of the emergent spectrum on the planet’s surface temperature. Spectra for planets with 1800, 1500, 1200, and 1000 K surface temperatures are plotted in purple, blue, green, and red, respectively, for a 1-bar solar-composition atmosphere.

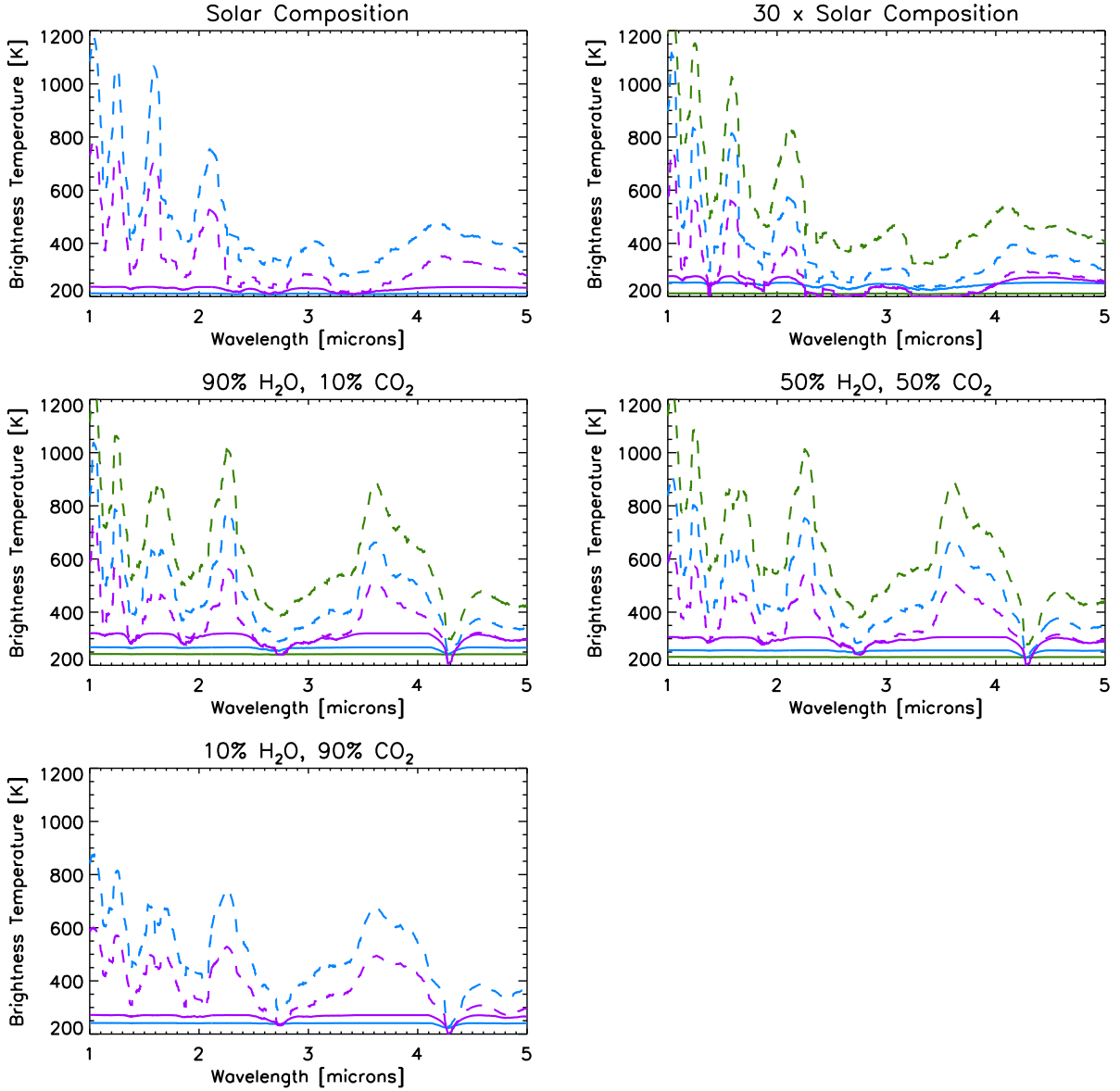


Fig. 5.— Emission spectra for hot super-Earths ($T_{surf} = 1500$ K) with cloudy and partially cloudy atmospheres. It is assumed that the clouds here are due to water condensation. Solid-lined spectra denote the case where the entire planet is blanketed by clouds, whereas the dashed lines indicate cases where the clouds only obscure 75% of the planetary surface. Planets with surface pressures of 10, 100, and 1000 bars are denoted by green, blue, and purple lines respectively. None of the 1-bar atmospheres are expected to have clouds owing to the fact that their temperature-pressure profiles do not cross the water condensation curve. Additionally, none of the Venus-composition atmospheres are expected to have water clouds for the same reason. The maximum brightness temperature for an atmosphere with thick water clouds is only 320 K. However, if clouds are patchy and obscure only a fraction of the planet, then the possibility exists to observe much higher brightness temperatures - potentially as high as 1200 K if the clouds only cover 75% of the planetary surface.

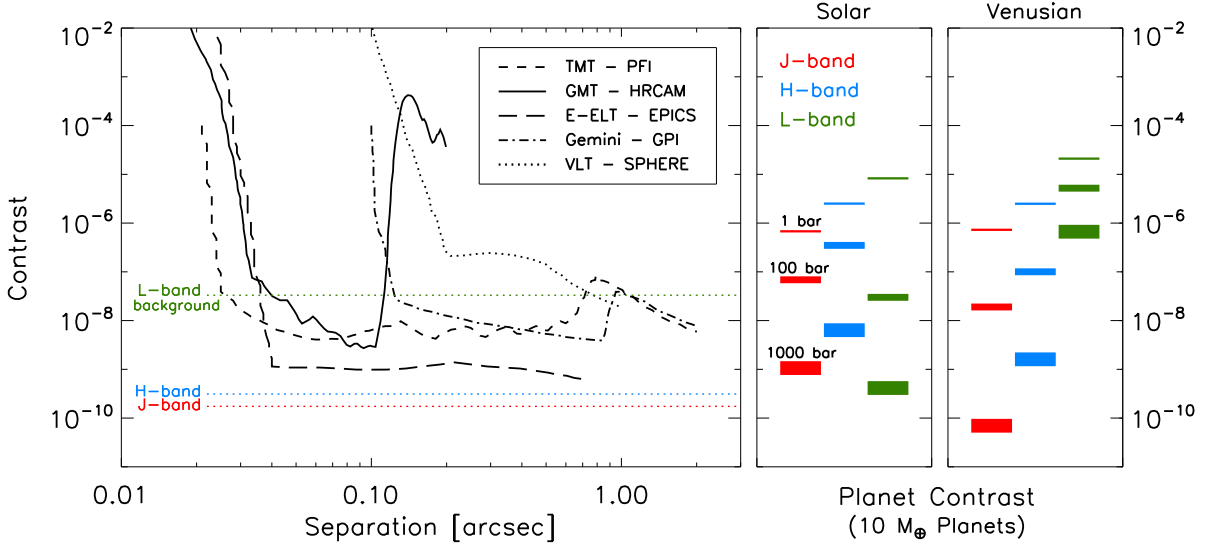


Fig. 6.— Left - Direct imaging contrast vs. angular separation for next generation exoplanet imaging instruments. Contrasts corresponding to the sky background for one-hour integrations for the GMT on a Sun-like star at 10 pc is overplotted in color (dotted lines) for J, H, and L band, showing that observations will be background limited at longer wavelengths. The sensitivity curves for the TMT’s planet imager PFI and Gemini’s GPI are from (Macintosh et al. 2006) for a 4th magnitude target in H-band. The curve for 1-hour exposures of HRCAM on the GMT is also for H-band (GMT Conceptual Design Report: <http://www.gmto.org/CoDRpublic>). Corresponding sensitivity curves for SPHERE on VLT and EPICS on E-ELT (Kasper et al. 2008) are instead shown at J-band. Right - Upper limits in contrast needed to detect hot protoplanet afterglows with various atmospheric masses. The upper limits shown here are for the detection of $10 M_{\oplus}$ planets ($T_{surf} = 1500$ K) with solar- and Venus-composition atmospheres (composition cases 1 and 6) orbiting a solar-type star. The line weights denote the planet’s atmospheric surface pressure - 1 bar (thin lines), 100 bar (medium-weight lines), and 1000 bar (thick lines). Limits for 10 bar atmospheres have been omitted to avoid confusion. Planet-star contrast levels for a $1 M_{\oplus}$ planet are a factor of $\sim 3 - 10$ lower than what is shown here for a $10 M_{\oplus}$ planet.